The evaporite shear zone of the Jura Boundary Thrust – New evidence from Wisen well (Switzerland)

By Peter Jordan, Thomas Noack and Thomas Widmer[1])

ABSTRACT

At Wisen well, the Aniso-Ladinian Muschelkalk evaporites form a ca. 30 m thick thrust zone separating the Mesozoic carbonate thrust sheet of the Jura from the Miocene conglomerates of the footwall. The shear zone documents ca. 4.8 km of transport, a significant decrease in thickness normal to the shear zone and a late 45° clock-wise rotation of transport direction. It comprises four deformation units: An upper dolomite fault breccia, folded shale-sulfate multilayers, anhydrites with distinct flow structures, and a lower fault breccia melange with exotic blocks from the footwall («Aufgeschürfte Massen»). While the lower part is completely overprinted, a correlation of the upper part with other Muschelkalk sequences of northern Switzerland may still be possible. The shale-sulfate multilayers and the anhydrites show well-organized deformation structures like foliation, stretching lineation, flow folds (with some folds having axes parallel to stretching lineation), asymmetric boudinage and pressure shadows. Despite of the low temperatures (≤ 70 °C) and the high strain rates (ca. $1 \cdot 10^{-13}$s^{-1}), intracrystalline glide and twinning were the dominant deformation mechanisms in anhydrite. Tectonically induced twinning of calcite is found in the exotic footwall blocks in the lower fault breccia melange.

ZUSAMMENFASSUNG

Die Muschelkalkevaporite («Anhydritgruppe», Aniso-Ladinian) der Bohrung Wisen SO bilden den etwa 30 m mächtigen Abscherhorizont der Jura Randüberschiebung. Dieser lässt sich hier in vier Deformationsbereiche unterteilen: 1) Eine obere, vorwiegend dolomitische, tektonische Brekzie, 2) duktil verfaltete Ton-Sulfat-Wechsellagerungen, 3) massive Anhydrite mit Fliessfalten und 4) eine untere tektonische Brekzie mit exotischen Blöcken («Aufgeschürfte Massen»). Während der obere Teil noch relativ gut mit benachbarten undeformierten Profilen korreliert werden kann, macht die penetrative Verscherung des unteren Teils eine stratigraphische Korrelation höchst spekulativ. Dennoch kann gezeigt werden, dass die Anhydrithorizonte auf bis zu 35% der ursprünglichen Dicke ausgedünnt wurden und dass die Salzlager komplett verschwunden sind. In den Ton-Sulfat-Wechsellagerungen und den massiven Anhydriten dokumentieren Schieferung, Streckungslineation, Fliessfalten, asymmetrische Boudinage und Druckschatten eine klar organisierte Deformation. Einige der Faltenachsen wurden in Richtung der Streckungslineation abgelenkt. Stark gelängte Anhydrite zeigen, dass trotz tiefen Temperaturen (≤ 70 °C) und hohen Scherraten (ca. $1 \cdot 10^{-13}$s^{-1}) intrakristallines Gleiten und Verzwillingung in Verbindung mit Korngrenzwandern die wichtigsten Verformungsmechanismen waren. Duktile Verformung kann auch im Kalzit (Verzwillingung) und Gips nachgewiesen werden. In der Haupttransportrichtung (NNW) kann aus der Profilkonstruktion eine Verkürzung von ca. 4,8 km ermittelt werden. Eine vorwiegend spröde Überprägung dokumentiert jedoch eine späte Ablenkung der Transportrichtung nach NNE.

[1]) Geologisch-Paläontologisches Institut der Universität, Bernoullistrasse 32, CH–4056 Basel (Switzerland).

Introduction

In the summer of 1988, the Jura boundary thrust, an evaporite detachment horizon was fully recovered in a core of the Wisen well providing the most spectacular document of an evaporite shear zone ever seen within the Jura. The well RB 29 located NE of Wisen village (Swiss coordinates 634 546/249 947) (Fig. 1) was drilled by the Swiss Federal Railway (SBB) in the context of the projected "Wisenberg-Tunnel" (STEINER 1989). Drilling started in the "Hauptmuschelkalk"-limestones. The underlying Aniso-Ladinian Muschelkalk evaporites ("Anhydritgruppe", c.f. DRONKERT 1987; WIDMER 1989), the main decoupling horizon of Jura overthrusting (e.g. LAUBSCHER 1961; JORDAN & NÜESCH 1989a), was first encountered at 24.4 m, the siliciclastical Miocene sediments of the footwall were reached at 63.2 m. Drilling was stopped at 284.6 m (KOCHER & TAFERNER 1989). The evaporite sequence was investigated from a sedimentological, stratigraphical and structural point of view at the drill site.
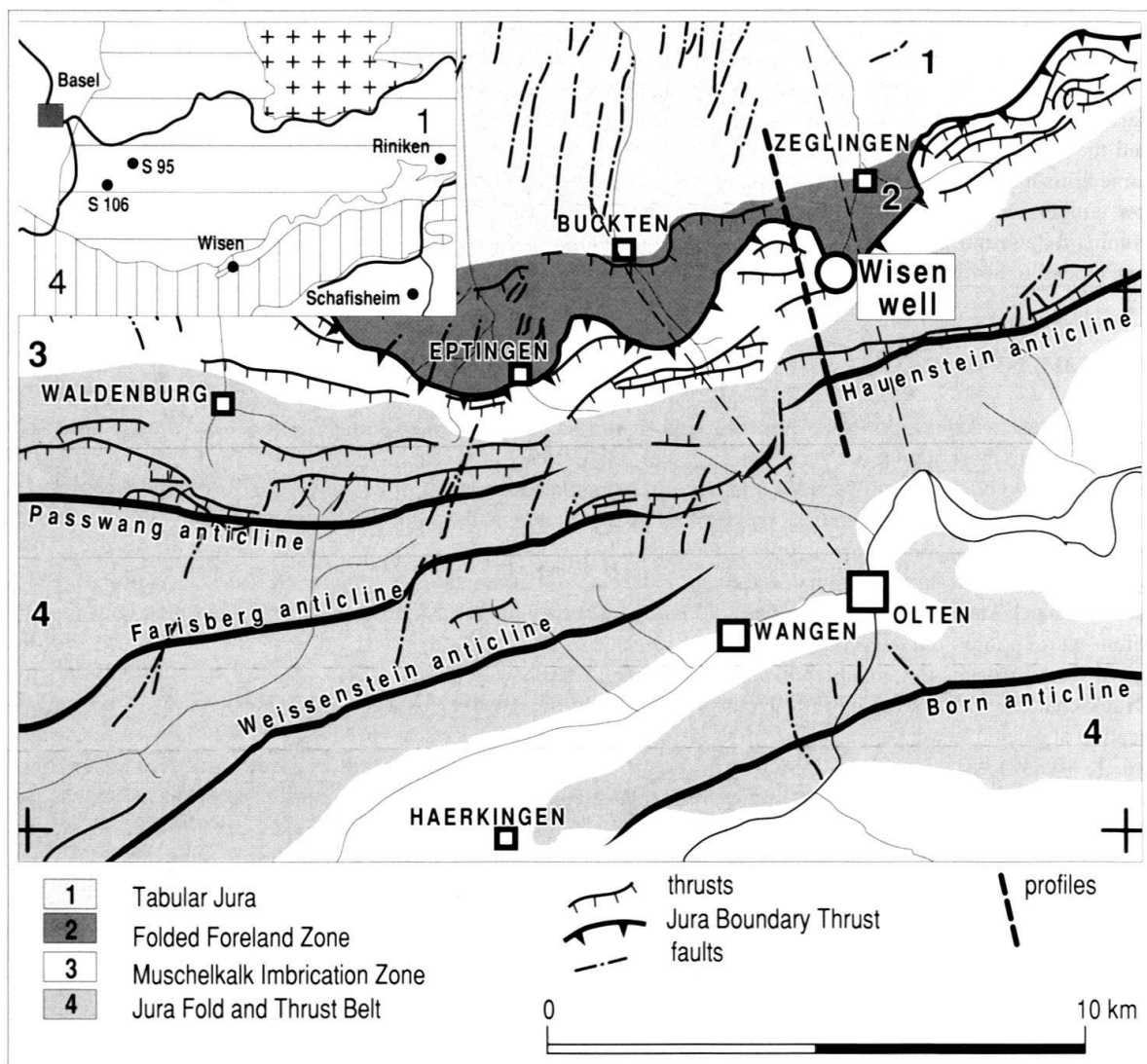

Fig. 1. Tectonical overview of the surroundings of Wisen well (based on MÜLLER et al. 1984 and recent mapping). The small map shows the location of the referenced wells.

Additionally, 17 core samples were selected for further investigation by thin section analysis, X-ray diffractometry, X-ray texture goniometry, scanning electron microscopy (SEM) and X-ray spectrometry (EDX).

Tectonical setting

The N-S trending cross-section "Wisenberg" (NOACK 1989) (Fig. 2), located about 400 m west of Wisen well gives an overview of the different tectonical units near the well (c.f. Fig. 1). From North to South, the cross-section cuts across the following units:

1. The *Tabular Jura* (north of the Hofmatt), with a regional dip of 3–5° south, was affected by NNE-SSW to NE-SW trending normal faults attributed to the Oligocene Rhine graben system (e.g. BUXTORF 1901). It was not visibly affected by the Late Miocene compression.

2. The *folded foreland zone* ("Vorfaltenzone", Fig. 1) was slightly shortened by folding and thrusting and is located to the North and underneath the Jura boundary thrust. For the construction of the "Wisenberg" cross-section, the Sprüssel anticlines that are documented in the Hauensteinbasistunnel further to the East (Fig. 1; e.g. BUX-TORF 1916; LAUBSCHER 1977) were laterally projected into the cross-section. These two small anticlines document a shortening of ca. 100 m. Further to the West, they lead into the fairly uniformly WNW-ESE striking Homberg thrust with the shortening increasing to about 750 m (Fig. 1). Kinematical considerations suggest that this zone has been formed before the main Jura overthrusting event that resulted in the Jura boundary thrust (NOACK 1989).

3. The *Muschelkalk imbrication zone* ("Muschelkalk Schuppenzone", Fig. 1) represents in this part of the Jura the frontal zone of Jura boundary thrust. Four to six imbrications formed by Middle Triassic carbonates and evaporites, i.e. the lowermost formations involved in Jura detachment were thrust onto the Miocene footwall. Laterally, they can be grouped into several segments of different strike and width. At the "Wisenberg" the cumulative shortening by imbrication amounts to about 800 m. The total displacement at the Jura boundary thrust proper is about 4.8 km.

4. The *Jura fold and thrust belt* ("Faltenjura", Fig. 1) is overthrust as an entity on the Tabular Jura (Jura boundary thrust) and, additionally, it shows strong internal overthrusting and folding. The Hauenstein anticline in the Wisen cross-section represents a kind of a fault-propagation-fold (SUPPE 1985) related to the Dottenberg thrust with about 1.3 km of thrusting (for a detailed kinematical model of the Dottenberg thrust see LAUBSCHER 1983). Further to the West, the anticline is faulted and sinistrally displaced by about 600 m into the Farisberg anticline. In a map view (Fig. 1), there is a change in strike of the Jura front and the Boundary thrust from NE-SW to E-W.

The location of these thrusts were apparently triggered by underlying flexures in the detachment zone that act as stress concentrators (NOACK 1989; BITTERLI & NOACK 1989). Further to the East, on the evidence of the seismic lines of Nagra (LAUBSCHER 1986) they seem to be due to Tertiary reactivation of the border faults of the underlying Paleozoic troughs ("Nordschweizer Permokarbontrog", e.g. DIEBOLD 1983; LAUBSCHER 1987). These observations can be extrapolated to the west in order to explain these flexures in the basement (NOACK 1989).
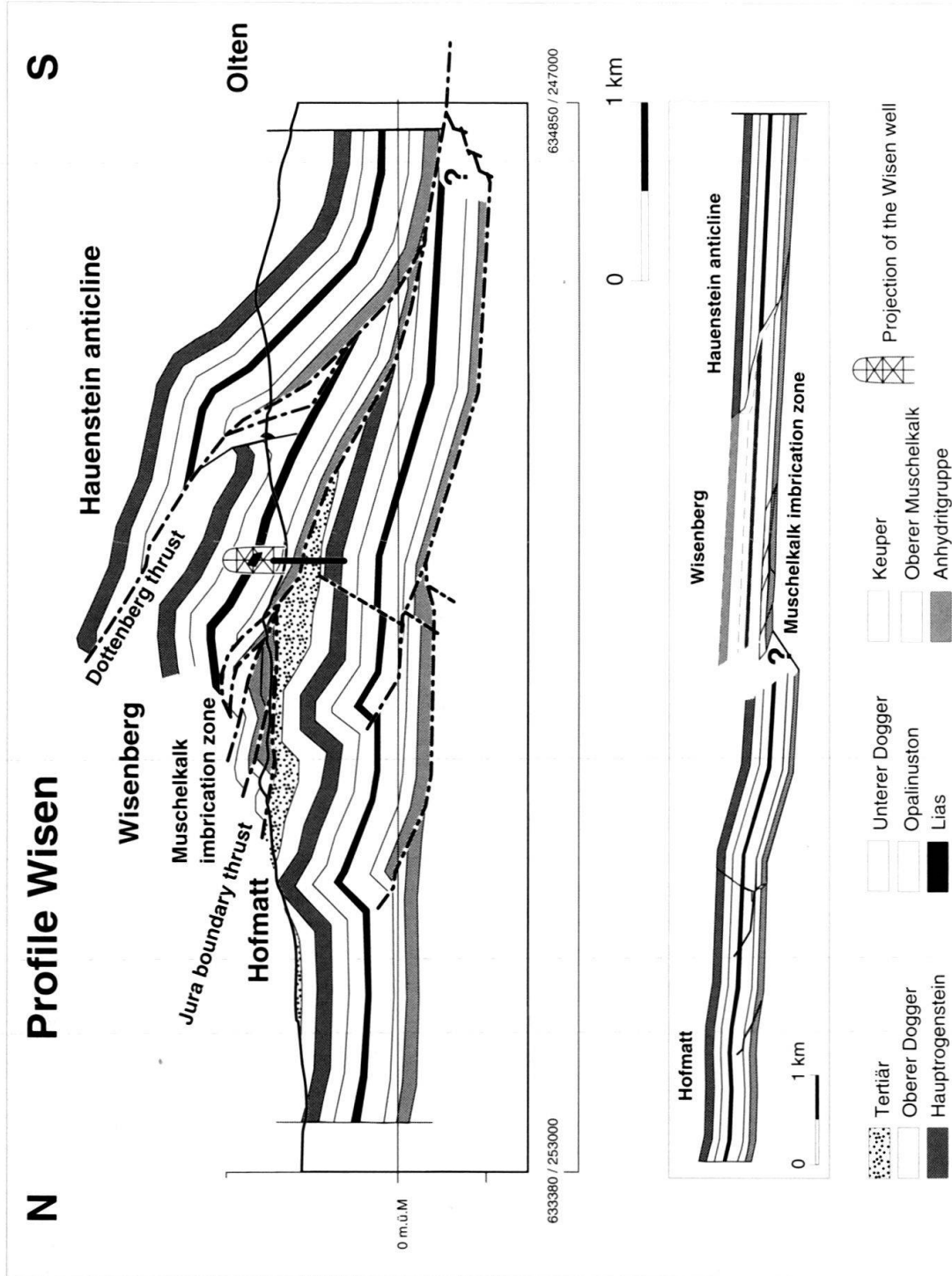
Fig. 2. Wisenberg cross section (about 400 m West of the Wisen well, c.f. Fig. 1) and restored section (bottom), constructed and balanced using Geosec-20™, Copyright © Geo-Logic Systems, Inc 1989.

The total amount of overthrusting and internal shortening in the "Wisenberg" cross-section sums up to about 6.2 km.

Description of the core

Figure 3 gives an overview of the petrology, the mineralogy and the deformation structures of the Muschelkalk evaporites at Wisen well. As expected from the tectonical situation, the most remarkable features are deformation structures. According to the nature of deformation, the evaporite shear zone can be subdivided into four deformation units:

32.6–37.0 m UPPER FAULT BRECCIAS: mainly dolomite fault breccias with some subordinate gypsum fault breccias in between and at the bottom.

37.0–ca. 51.0 m UPPER DUCTILE DOMAIN characterized by recumbent open folds: shale-anhydrite multi-layers and, subordinately, some thicker anhydrite beds, yet for the most part gypsified. Early ductile flow of anhydrite is still documented in relic grains. Strained gypsum documents syntectonical onset of gypsification (down to ca. 47 m) and ductile flow of gypsum thereafter. Dolomite layers are boudinaged. Dolomite-shale fault breccia occurs at 42.7–43.3 m. Sedimentary sulfate breccia (50.0–51.0 m) became a compact and foliated rock due to ductile overprint.

Ca. 51.0–59.1 m LOWER DUCTILE DOMAIN characterized by recumbent isoclinal folds: anhydrites with subordinate shale-anhydrite multilayers and nodular anhydrites. Flow folds in anhydrite and strongly elongated nodules document high strains. Sedimentary sulfate breccia (at 54 m) is strongly overprinted. At the bottom, anhydrite is partly overgrown by postkinematical gypsum.

59.1–63.2 m LOWER FAULT BRECCIAS: fault breccia melange comprising fragments of Muschelkalk evaporites and exotic blocks embedded in secondary gypsum matrix. Exotic blocks have obviously been scraped from the footwall during overthrusting ("Aufgeschürfte Massen", MÜHLBERG 1908). A Liassic arenitic limestone block (sample 13, Fig. 3) has been carried away more than 2 km along the thrust plane (c.f. Fig. 2).

Lithostratigraphical Correlation

Due to increasing deformation, the sedimentological features are increasingly obliterated with increasing depth. Nevertheless, some stratigraphical units can still be recognized, and *in broad terms,* the Wisen sequence can be correlated with the Muschelkalk evaporite sequences of the Vereinigte Schweizerische Rheinsalinen wells S 95 and S 106 (WIDMER 1989) and the Nagra wells Riniken and Schafisheim (DRONKERT et al. 1990) (Fig. 1). Below ca. 50 m, however, deformation is so pervasive that only suggestions about former lithofacies can be made.

In Fig. 4, the lithological sections in question are simplified and stilistically adapted to each other, while the two differing stratigraphical subdivisions of the formation (WIDMER 1989 and DRONKERT et al. 1990, respectively, c.f. Table 1) are indicated on both sides of the columns. This compilation does not stress whether the sulfates occur as anhydrite or gypsum as this is mainly a function of overburden and accessibility of water and it is therefore not meaningful for stratigraphical correlation.

The uppermost part of the Muschelkalk evaporites ("Anhydritgruppe"), the "Anhydritdolomit" (unit 10 of WIDMER 1989; for correlation with units of DRONKERT et al. 1990 see Fig. 4 and Table 1) consists of light colored beige dolomites of sub- to intertidal origin. They are either laminated (partly stromatolitic) or bioturbated and usually contain sulphate or chert nodules. This part is easily identified in the Wisen core, where it reaches down to a depth of 31.90 m.
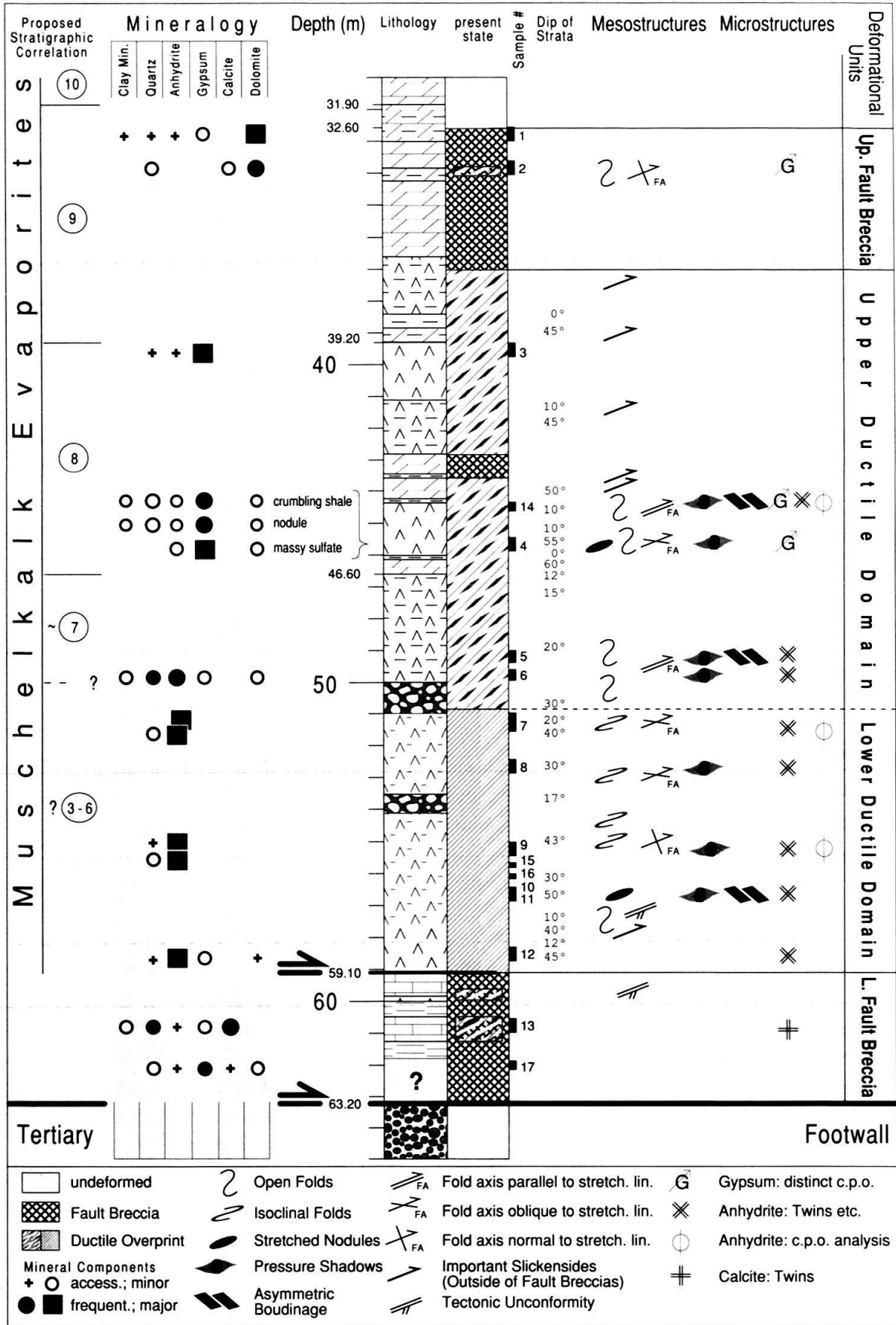
Between 31.90 m and 39.20 m, the Wisen core consists of beige, subtidal, biotu-
bated dolomites together with grey-brown, finely laminated dolomicrites of supratidal
origin at the top and an interval of grey-brown, laminated anhydrite with dolomitic
marls at the bottom. The finely laminated dolomicrites tend to be intensively brecci-
ated, so none of the typical sedimentary features such as intraformational flat pebble
conglomerates or dessiccation cracks can be observed. This part of the Wisen core is
best correlated with unit 9.

Light colored milky-white anhydrite, anhydrite-shale multilayers, beds of strongly
brecciated dolomicrites and marly intercalations are found between 39.20 m and
46.60 m. Despite the intense deformation of this horizon, characteristic beds of
massive dolomicrite give good evidence for a correlation with unit 8. Unfortunately,
neither fossils (characteristic for the bottom bed of unit 8) nor the well known cross-
bedded oolithes (in the upper part of unit 8) have been recognized at Wisen.
Supratidal, finely laminated dolomicrites are lacking as well. Nevertheless the light
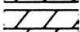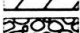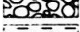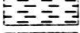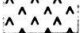colored anhydrite at the top is well developed in all cores.

The lower, strongly sheared part consists mainly of banded or laminated anhydrite
which changes in colour from milky white to dark brown-grey. Deformation is so per-
vasive that the original lithofacies can only be guessed. Nevertheless, the anhydrite
sequence between 46.60 m and 50.00 m resembles unit 7, although the selenitic
marker bed of the normal stratigraphical record, which is expected at this level, is mis-
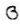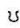sing at Wisen.

Two thin, marl-rich intervals at about 50 m and 54 m respectively, yet pervasively
foliated, still resemble sedimentary conglomerates or breccias. In undeformed sec-
tions, it is evident that breccias are mostly formed by solution of halite and collapse of
overlying strata. Conglomerates and breccias thus indicate ephemeral saline pond and
mud flat environments fringing the halite facies. They are contemporaneous with
deposition of halite and tend to cover it in the course of the two regressive cycles (units
1–3 and 4–6). Some of the massive anhydrites beneath the two breccia intercalations
in the Wisen core contain stretched reddish nodules which often occur in units 3 and 6.
Quartz, feldspar and mica detritus found in some thin sections of this zone are indica-
tive of former anhydrite-shale multilayers which are the main lithologies of units 3 and
6 and to a lesser degree of unit 4. So it is probable that most former conglomerates and
breccias were converted to massive anhydrite by tectonic overprinting. Another hypo-
thesis, the correlation of the breccias with units 3 and 6, and, as a consequence, corre-
lation of the lowermost anhydrite with the "Untere Sulfatzone" (unit 1) can be ruled
out because of the absence of any dolomites in this part of the Wisen core.

In short, the upper, lithologically heterogeneous parts of the Muschelkalk eva-
porites of Wisen well can be easily correlated with the other cores while the lower,

Fig. 3. Core section of the evaporite detachment at Wisen well: Depth is below surface at 630.55 m above s.l. Litho-
logical patterns refer to suggested initial (i.e. prekinematical) lithologies and are explained in Fig. 4. Below 62 m,
melange is so heterogeneous that no statements about the initial lithology can be made. Bars and numbers adjacent
to column refer to sample localization. Meso- and microstructure symbols are explained at bottom. Proposed litho-
stratigraphical correlation to the units by WIDMER (1989) is indicated at the left. Top of member 10 is at 25.4 m.
Below 47 m, deformation is so pervasive that the correlation is highly hypothetical.
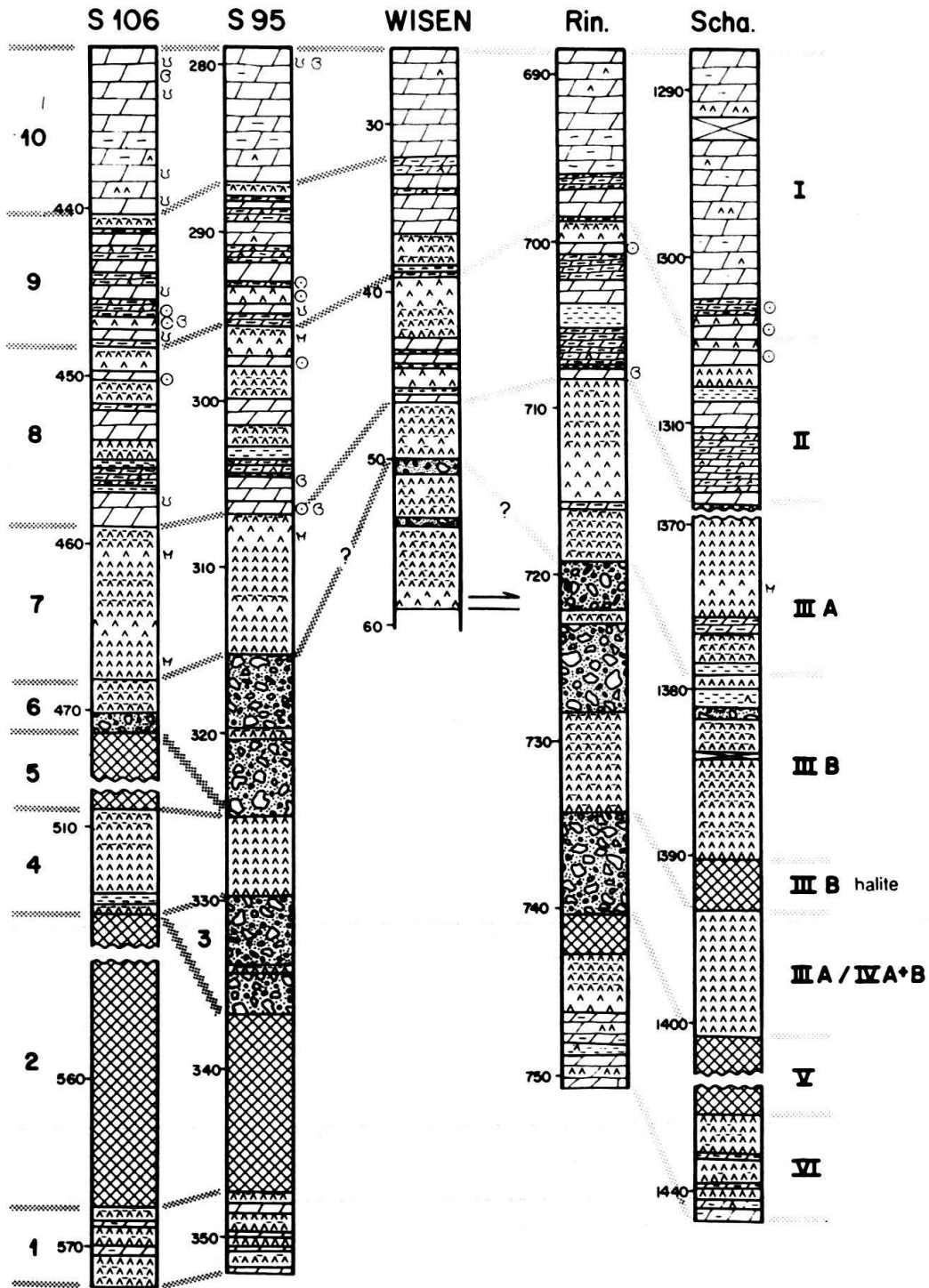
finely laminated dolomicrite	anhydrite-shale multilayers
massive dolomicrite to doloarenite	halite
evaporite conglomerates and breccias (sedimentary)	ooids
clays and dolomitic marls	fossils in general
light-colored, white to grey anhydrite	bioturbation
dark, grey to brown anhydrite	selenite bed

	Widmer (1989)	Dronkert et al. (1990)
10	"Anhydritdolomit"	I
9	"Dolomit dominierte Schichten"	
8	"Uebergangsschichten"	II
7	"Obere Anhydritschichten"	III A
6	"Obere Brekzien"	III B - IV
5	"Obere Salzschichten"	
4	"Untere Anhydritschichten"	
3	"Untere Brekzien"	
2	"Untere Salzschichten"	~ V
1	"Untere Sulfatzone"	VI

Tab. 1: Proposed correlation of the lithostratigraphic units given by WIDMER (1989) and DRONKERT et al. (1990), compare Fig. 4.

sulfate-rich parts are difficult to ascribe to the known stratigraphical units. Units 1, 2 and 5 are definitely lacking, and there is no doubling of any parts of the section.

Deformation Structures

Mesostructures

Deformation comprises ductile flow of anhydrite and gypsum, flow of shale-gypsum multilayers *(shale-gypsum tectonites,* JORDAN & NÜESCH 1989b), sliding on discrete slickensides, as well as fault brecciation. There is a clear indication from overprinting relationship that ductile flow of anhydrite preceded the onset of gypsification[2]), and, therefore, the ductile deformation of gypsum and the formation of shale-gypsum tectonites. The fault brecciation at the top of the sequence is in turn younger than the formation of shale-gypsum tectonites since relics of the latter are found within the breccias. Throughout the core, slickensides in shales have formed at all stages of the deformation history. Slickensides within pure anhydrite can be correlated to the youngest stages of deformation.

Ductile flow in anhydrite produced a distinct lineation L_1 that is defined by grain elongation, preferred orientation of rigid inclusions and pressure shadows. Within the

[2]) Additional ductile flow of halite has to be assumed simultaneously to the flow of anhydrite. However these halite layers must have been completely dissolved before the onset of gypsification, as high Na-Cl contents in solution prevents anhydrite from gypsification (e.g. HARDIE 1967; PRIESNITZ 1969).

Fig. 4. Lithostratigraphical correlation of Wisen Muschelkalk evaporite sequence with wells S 106 and S 95 (Vereinigte Schweizerische Rheinsalinen) and Nagra-wells Riniken (Rin) and Schafisheim (Scha) (WIDMER 1989 and DRONKERT et al. 1990, respectively). For well sites see Fig. 1. The lithostratigraphical units by WIDMER (1989) and DRONKERT et al. (1990) are indicated on the left and right side, respectively.

anhydrites of the lower ductile domain, a pronounced C foliation has developed whereby C is more or less parallel to the original layering.

Flow in anhydrite resulted in asymmetrical open Class 1C to Class 2-folds (RAMSAY 1967) as well as in recumbent isoclinal similar (Class 2) folds. The latter are restricted to the thicker anhydrite sequences, while open folds are found also within shale-sulfate multilayers (Fig. 3). Independent of the fold shape, some fold axes are *perpendicular* to stretching lineation L_1 (Fig. 5a) while others are successively deflected towards L_1 until they are *parallel* to stretching lineation (Fig. 5b, c.f. Fig. 3). This deflection is indicative for high strains. Sheath folds as mentioned from other evaporite shear zones (MARCOUX et al. 1987; HARLAND et al. 1988; MALAVIEILLE & RITZ 1989), however, have not yet been unambiguously recognized at Wisen.
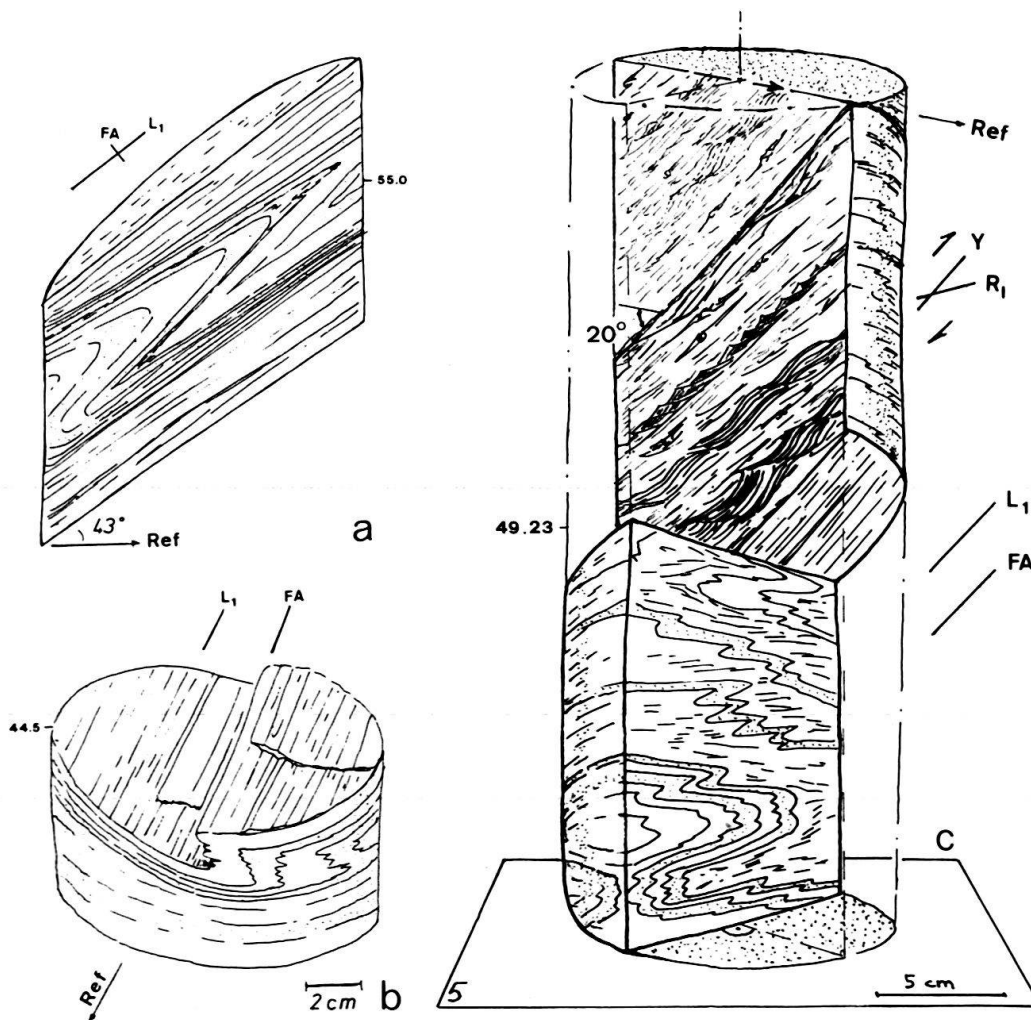
Fig. 5. Folds: a) Isoclinal recumbent similar fold in massive anhydrite (sample 9) with fold axes (FA) perpendicular to stretching lineation (L_1). b) Open similar fold in sulfate with thin shale interlayers (sample 14). FA is parallel to L_1. c) Sketch displaying the two-face nature of the shale-sulfate multilayers in sample 5. Top core is cut parallel to L_1 and shows Y-R structures and antithetically rotated pull-aparts. Bottom core is cut normal to L_1 and shows recumbent isoclinal Class 1C-folds with FA parallel to L_1. The interface between two cores is formed as shale slickenside. Ref.: Reference direction (c.f. Fig. 7).

A pronounced Y-R fabric (LOGAN et al. 1976) has developed within the shale-sulfate multilayers of the second deformation unit that are at the same time severely folded parallel to L_1 which results in the characteristic two-face nature of this unit (Fig. 5c). The Y-R fabric is formed by normal fault extensional shear bands (R, c.f. *ecc* of PLATT & VISSERS 1980) and shear zones parallel to the shear zone boundary (Y). The more competent and brittle shale interlayers are boudinaged along synthetical shear surfaces (X'_α) and form lozenge-shaped (asymmetric) and antithetically rotated pull-aparts (JORDAN 1991). These pull-aparts are also common in the domain of the stretched nodular anhydrites (sample 11) (Fig. 6a). The antithetical rotation of these pull-aparts documents a significant shortening normal to the thrust plane (JORDAN 1991).

Slickensides have formed from the initial stages of deformation (ductile flow of anhydrite) until the latest movements within the fault breccias. At the initial stages, slickensides developed preferentially within the (brittle) shale interlayers and sliding direction was parallel to the stretching lineation L_1 of anhydrite (Fig. 7, c.f. Fig. 5 a, b). These slickensides are overprinted obliquely by later slickensides (L_2) documenting a 45° change in transport direction after anhydrite left the ductile field. The clock-wise rotation of transport direction is documented throughout the whole core section: i) by late (shale-free) slickensides in pure anhydrite (e.g., in sample 12), ii) by the growing direction of some gypsum fibres in veins that is slightly deflected from L_1 towards L_2 (Fig. 7b), and iii) by pressure shadows. Antitaxial anhydrite and gypsum pressure shadows predominantly formed adjacent to shale clasts (Fig. 6b) and rarely adjacent to dolomite porphyroblasts. Some of the pressure shadows consist of distal (older) anhydrite fibres and proximal gypsum fibres, demonstrating that growth of these pressure shadows has started in the stability field of anhydrite and went on after gypsum became stable.

Microstructures

The anhydrite of samples 5–12, and 14 (i.e., the interval between ca. 44–59 m, Fig. 3) shows distinct crystal (lattice) preferred orientation (c.p.o.) and preferred grain shape orientation. The microstructures correspond qualitatively to those already described from the Belchen tunnel (JORDAN 1988), but the present samples document distinctly more intense deformation. Optically, the most conspicuous feature is twinning (Fig. 6c). Additionally, undulous extinction, formation of subgrains and grain boundary migration can be observed. Grains are distinctly elongated in the direction of the mesoscopical lineation, but almost equi-dimensional in a section normal to lineation (uniaxial constriction up to 10:1:1). There is also some evidence for grain size reduction by subgrain rotation.

As even complete twinning of a favourably oriented anhydrite produces only very little strain (RAMEZ 1976; MÜLLER et al. 1981), other mechanisms have to be responsible for the distinct elongation of the anhydrite grains. MÜLLER et al. (1981) suggest translation glide on $(001)[010]$, $(012)[1\bar{2}1]$ and $(012)[1\bar{2}\bar{1}]$ (in combination with grain boundary migration as recovering mechanism) to be the most important deformation mechanism of anhydrite creep at low temperatures and high strains. As this mechanism results in deformation bands and subgrains, the corresponding features of Wisen can
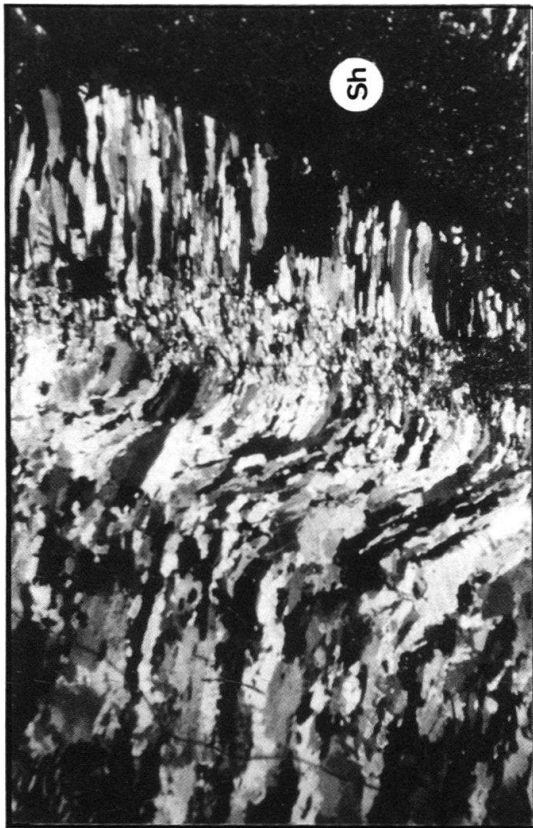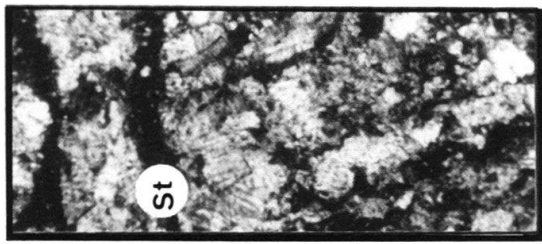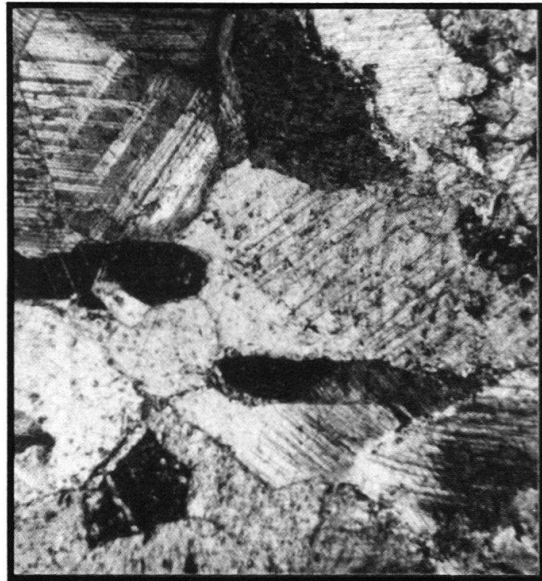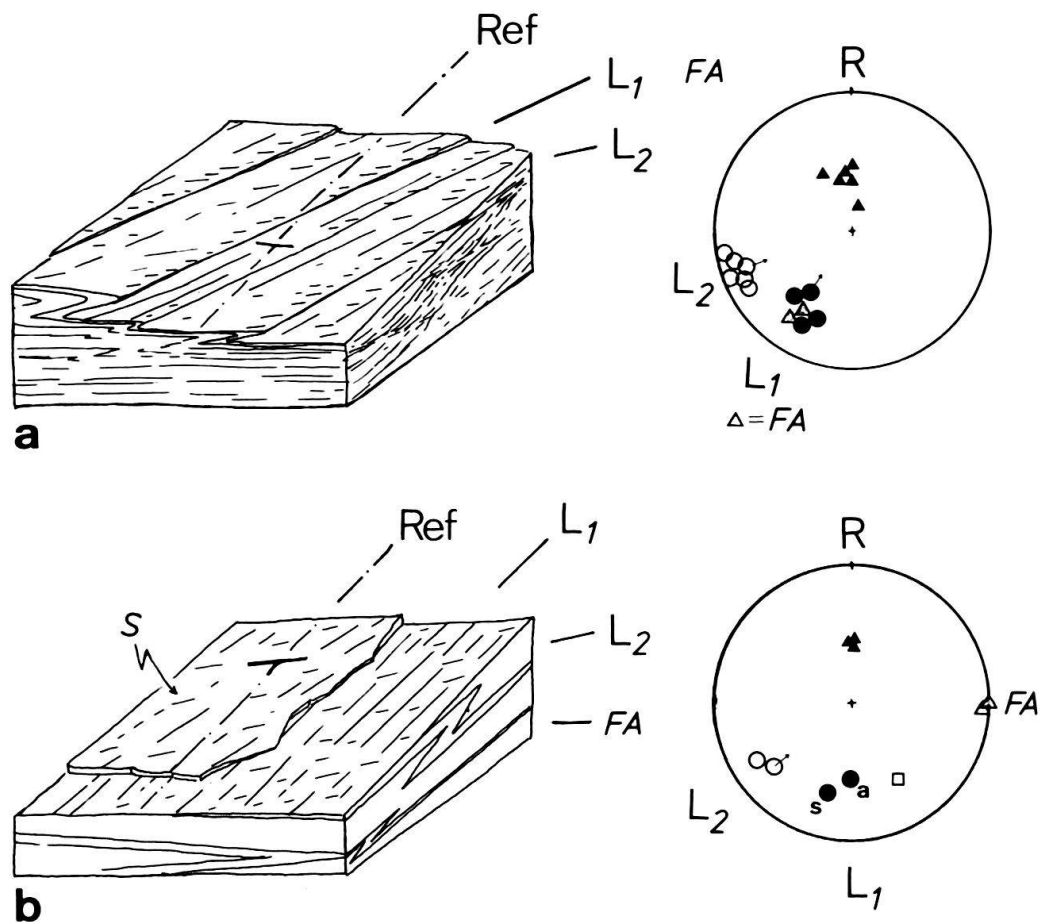
Fig. 7. Sketch and pole figure showing the clockwise rotation of transport direction in time: Reference R is the projection to horizontal of the dip line of the top layer of an intact core sequence and points to the opposite direction than dip direction. This reference has to be used as the cores are not oriented. Triangles are foliation poles, squares are FA, dots are L_1, open circles are L_2. Small arrows indicates transport direction of the hangingwall. Measurements from sample 7 (a), and sample 9 (b). Throughout the whole evaporite section the angle between L_1 and L_2 counts some 45° in a clock-wise direction while the orientation of the two lineation relative to reference line is not consistent.

be interpreted as indication for the presence of intracrystalline glide. This is also supported by the c.p.o. patterns (Fig. 8) that show distinct maximum of the pole to (210) around the lineation trace (dominant in Fig. 8a) and/or in the plane of foliation (dominant in Fig. 8d). The combined reflex of the poles to (020) and to (002) shows maxima almost parallel to lineation and normal to foliation. Additionally, there is a characteristic girdle normal to lineation (e.g. Fig. 8b) and/or a maximum normal to lineation

Fig. 6. Micrographs (b and c: ultra thin sections [<10 μm]): a) Antithetically rotated shale pull-aparts in anhydrite: bulk vorticity is clockwise while the rotation of the antithetically rotated pull-aparts (AR) is anti-clockwise (sample 11). b) Anhydrite fibres in the pressure shadow of a shale clast (Sh) showing rotation in extension (transport) direction (sample 5, section parallel to foliation, arrow indicates reference direction (c.f. Fig. 7)). c) Flow of anhydrite: Twinning, formation of subgrains (notice indications for grain size reduction) and grain boundary migration in uniaxially constricted anhydrite (sample 7). d) Tectonically induced calcite twins in coarse-grained vein (left) and fine-grained matrix. St.: Stylolithe seam (sample 13).
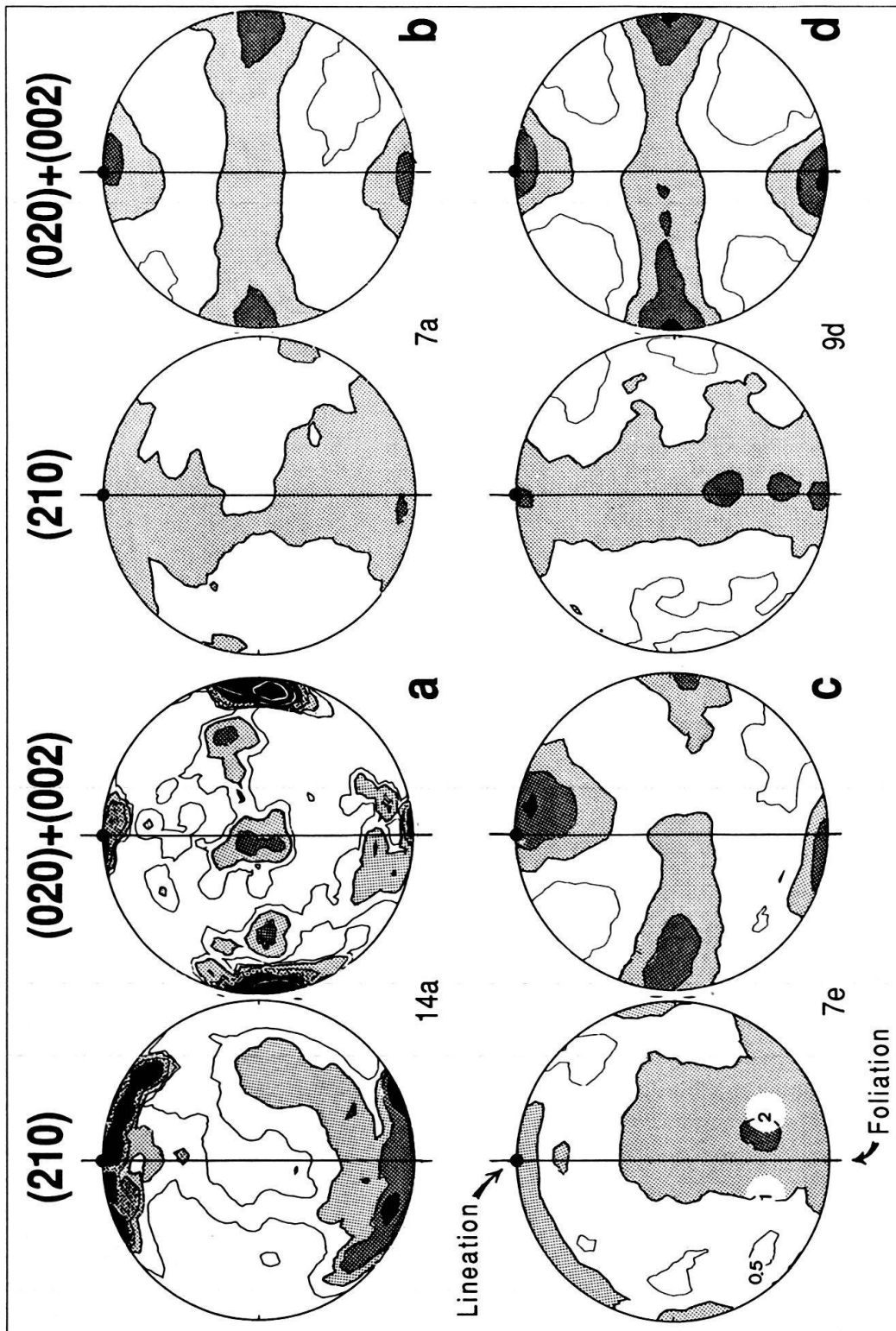
Fig. 8. Anhydrite c.p.o: (210) and combined (020) and (200) reflex pole figures from samples originating from 44.5 m (a), 51.3 m (b), 51.4 m (c) and 52.8 m (d). a) c.p.o. of relic anhydrite grains in gypsified shale-sulfate multilayer shown in Fig. 5b. b–d) pure anhydrite layers. Normal to foliation S trends E-W, lineation L_1 is vertical, shear is dextral. Contour intervals: 0.5, 1, 2, 4, 8 and 16 times uniform distribution, area <1 is white, 1–2 light grey, 2–4 dark grey, >4 black.

(e.g. Fig. 8a). Similar patterns are common throughout the Jura evaporite shear zones, however they diverge from published anhydrite patterns (domal anhydrite, LAMKE 1936; experimentally deformed anhydrite, MÜLLER et al. 1981; and sedimentary anhydrite, SCHWERDTNER 1961).

Within the Upper Ductile Domain, distinct c.p.o. and moderate to distinct elongation of gypsum document ductile flow after syntectonical gypsification. This syntectonical gypsification reaches down to ca. 46 m, present gypsification front is at ca. 50 m. All gypsum samples show grain boundary migration and recrystallization (growth of idiomorphic granoblasts). However, these two processes are common within all gypsified rocks (e.g. HOLLIDAY 1970) and, at this place, they rather document postkinematical recrystallization than flow up gypsum. Twinning as suggested by BAUMANN (1984) to be an important deformation mechanism of gypsum has not yet been recognized at Wisen.

The calcite of the exotic block of Lias (sample 13, Fig. 3) shows in the matrix as well as in the veins tectonically induced twinning (Fig. 6d) to an extent that has not been recognized within this part of Jura before. (Commonly, pressure solution and cataclasis which are documented in sample 13 as well, are the dominant mechanisms of calcite deformation in Jura [e.g. LAUBSCHER 1979; DROXLER & SCHAER 1979]). This pervasive twinning documents high differential stress concentrations (e.g. ROWE & RUTTER 1990) that possibly occurred during scraping or when the block was jammed during transport.

Discussion and Conclusions

At Wisen, movements along the Jura boundary thrust that is localized within the Muschelkalk evaporites amount to some 4.8 km. At an initial stage, strain was mainly accommodated by ductile flow of anhydrite, while at a later, sub-surface stage, main shear movements changed into new-grown gypsum and finally to fault breccias. The rock-salt members of the Muschelkalk Evaporites (units 2 and 5 of WIDMER 1989), an important lubricant of the Jura décollement in the hinterland are completely absent at Wisen, probably due to early synkinematical subrosion. The members where anhydrite dominates (units 3, 4, 6, 7), are reduced to less than 35% compared to the average thickness of corresponding foreland and hinterland sequences (Fig. 4) documenting an important shortening normal to the shear zone within the Jura boundary thrust (c.f. MALAVIEILLE & RITZ 1989). This compression is also documented by antithetically rotated pull-aparts and extension crenulation features within the anhydrite shear zone proper. The lithologically mixed member (unit 8) still shows some preserved sedimentary structures but is also clearly strained and slightly reduced in thickness (ca. 75% of standard thickness). The lower dolomite member (unit 9) and the dolomite interlayers within the anhydrite members are severely brecciated and boudinaged respectively while the upper dolomite member (unit 10) is nearly undeformed.

The Wisen core documents that ductile deformation in evaporite shear zones is not chaotic but rather well organized as already recorded from the other localities (LAUBSCHER 1975, 1984; MARCOUX et al. 1987; HARLAND et al. 1988; JORDAN 1988; MALAVIEILLE & RITZ 1989; JORDAN & NÜESCH 1989 a and b). Kinematical indicators give an adequate information on thrusting direction and its changes in time, as well as on

changes in shear zone geometry (e.g. compression normal to shear zone). Fold axes deflected towards transport direction and the completely extinguished sedimentological features document high strains of anhydrite.

Three differing mechanisms for anhydrite flow at low temperatures have been suggested so far (JORDAN 1989): 1) Intracrystalline glide and twinning associated with dynamical recrystallization by grain boundary migration (MÜLLER et al. 1981); 2) pressure solution and Bassanite lubrication (LAUBSCHER 1984); and, 3) deformation in the form of gypsum that is syntectonically dehydrated to anhydrite (BAUMANN 1984). Microstructures and c.p.o.-analysis of Wisen clearly support the suggestions of MÜLLER et al. (1981). Temperature ($\leq 70°$) and strain rate (ca. $1 \cdot 10^{-13}$ s^{-1}) estimates at Wisen (based on NAEF et al. 1985 and DIEBOLD & MÜLLER 1985, c.f. JORDAN & NÜESCH 1989b), however, point to the fact that the transition into intracrystalline plasticity has to be localized at temperatures distinctly lower than 80 to 100 °C as expected by MÜLLER et al. (1981). This is in accordance with the observations of van BERKELEN (pers. comm. 1989) in the Eureka fold-and-thrust belt (SCHWERDTNER et al. 1988) and from other localities in the Jura. It may be explained either by the assumption that activation energies relevant in natural deformation are lower than those obtained from experimental work or, alternatively, by the presence of deformation mechanisms other than intracrystalline plasticity such as grain size sensitive flow (c.f. grain size reduction in Fig. 6c) or pressure solution (LAUBSCHER 1984). No evidence for the third mechanism as proposed by BAUMANN (1984) was found at Wisen.

At top and bottom of the evaporite shear zone, fault breccias have formed after anhydrite left the ductile field. The localization of the breccias is not only controlled by lithology but also by water access from top (Muschelkalk limestones) and bottom (various footwall aquifers) that resulted in gypsification, swelling of clay minerals and reduction of friction (JORDAN & NÜESCH 1989b).

Kinematical indicators in ductile anhydrite and slickensides in shale and brittle anhydrite document a 45° clockwise rotation of transport direction in time. This change is probably related to the prominent change in strike of the Jura boundary thrust to the West of the cross-section (Fig. 1). East of the profile the thrust ramp is located further to the North than West of it. Resulting space problems have obviously been solved by a local change in thrusting direction.

Acknowledgments

REFERENCES

BAUMANN, W. 1984: Rheologische Untersuchungen an Gips. Eclogae geol. Helv. 77/2, 301–325.
BITTERLI, TH. & NOACK, TH. 1989: Tektonische Massenbilanz in der Profilebene und in der dritten Dimension – Konsequenzen für die Rekonstruktion der Sockeltektonik im Modellfall Basler Jura. NFP 20 Bulletin 8, 14.

BUXTORF, A. 1901: Geologie der Umgebung von Gelterkinden. Beitr. geol. Karte Schweiz (NF) 11.
— 1916: Prognosen und Befunde beim Hauensteinbasis- und Grenchenbergtunnel und die Bedeutung der letzteren für die Geologie des Juragebirges. Verh. Natf. Ges. Basel. 27, 184–254.
DIEBOLD, P. 1983: Der Permo-Karbon-Trog der Nordschweiz. Nagra informiert 5, 10–15.
DIEBOLD, P. & MÜLLER, W.H. 1985: Szenarien geologischer Langzeitsicherheit: Risikoanalyse für ein Endlager für hochradioaktive Abfälle in der Nordschweiz. NTB 84–26, NAGRA Baden.
DRONKERT, H. 1987: Diagenesis of Triassic evaporites in Northern Switzerland. Eclogae geol. Helv. 80/2, 397–414.
DRONKERT, H. & BLÄSI, H.-R. & MATTER, A. 1990: Facies and origin of Triassic evaporites from the Nagra boreholes, Northern Switzerland. Geologische Berichte (Landeshydrol. & -geol.) 12.
DROXLER, A. & SCHAER, J.-P. 1979: Déformation cataclastique plastique lors du plissement, sous faible couverture, de strates calcaires. Eclogae geol. Helv. 72/2, 551–570.
HARDIE, L.A. 1967: The Gypsum-anhydrite equilibrum at one atmosphere pressure. Amer. Mineralogist 52, 171–200.
HARLAND, W.B., MANN, A. & TOWNSEND, C. 1988: Deformation of anhydrite-gypsum rocks in central Spitsbergen. Geol. Mag. 125, 103–116.
HOLLIDAY, D.W. 1970: The petrology of secondary gypsum rocks: a review. J. sediment. Petrol. 40, 734–744.
JORDAN, P. 1988: Deformationsverhalten der Keuper Evaporite des Belchen-Tunnels (Faltenjura, Schweiz). Erlanger Beitr. Geol. 116, 53–66.
— 1989: Deformation mechanisms in naturally strained anhydrite. 28th Int. Geol. Congr. (Washington) Abstr. 2, 137–138.
— 1991: Asymmetric boudinage of shale interlayers in evaporite shear zones. J. struct. Geol. in press.
JORDAN, P. & NÜESCH, R. 1989a: Deformation structures in the Muschelkalk anhydrites of the Schafisheim Well (Jura Overthrust, Northern Switzerland), Eclogae geol. Helv. 82/2, 429–454.
— 1989b: Deformational behavior of shale interlayers in Evaporite detachment horizons (Jura Overthrust, Switzerland). J. struct. Geol. 7, 859–871.
KOCHER, R. & TAFERNER, A. 1989: Sondierbohrung RB 29 – Bohrprofil. – in: Wisenberg-Tunnel. Vorprojekt Geologie SBB und Ing. Gem. Wisenberg-Tunnel (Bern) (unpubl.).
LAMCKE, K. 1936: Gefügeanalytische Untersuchungen am Anyhdrit nebst einem Beitrag zu den optischen und röntgenoptischen Methoden der Gefüge-Analyse. Schr. mineral.-petrogr. Inst. Univ. Kiel, 4.
LAUBSCHER, H.P. 1961: Die Fernschubhypothese der Jurafaltung. Eclogae geol. Helv. 54/1, 221–282.
— 1976: Viscous components in Jura folding. Tectonophysics 27, 239–254.
— 1977: Fold development in the Jura. Tectonophysics 37, 337–362.
— 1979: Elements of Jura kinematics and dynamics. Eclogae geol. Helv. 72/2, 467–483.
— 1983: Überschiebungen im Jura. Jber. Mitt. oberrhein. geol. Ver. N.F. 65, 181–189.
— 1984: Sulfate deformation in the upper Triassic of the Belchen tunnel (Jura Mountains, Switzerland). Eclogae geol. Helv. 77/2, 249–259.
— 1986: The eastern Jura: Relations between thin-skinned and basement tectonics, local and regional. Geol. Rdsch. 73, 535–553.
— 1987: Die tektonische Entwicklung der Nordschweiz. Eclogae geol. Helv. 80/2, 287–303.
LOGAN, J.M., FRIEDMANN, M., HIGGS, N., DENGO, C. & SHIMAMOTO, T. 1979: Experimental studies of simulated gouge and their application to studies of natural fault zones. U.S, geol. Surv. Open-File Report 79–1239, 305–343.
MALAVIEILLE, J. & RITZ, J.F. 1989: Mylonitic deformation of evaporites in décollements: examples from the Southern Alps, France. J. struct. Geol. 11, 583–590.
MARCOUX, J., BRUN, J., BURG, J.-P. & RICOU, L.E. 1987: Shear structures in anhydrite at the base of thrust sheets (Antalya, Southern Turkey). J. struct. Geol. 9, 555–561.
MÜHLBERG, F. 1908: Erläuterungen zur geologischen Karte der Umgebung von Aarau. Geol. Karte Schweiz, Spez. Karte 45.
MÜLLER, W.H., PASQUIER, F. & HUBER, M. 1984: Geologische Karte der Nordschweiz 1:100 000. Geologische Spezialkarte 121. Basel (Schweiz. Geol. Komission).
MÜLLER, H.W., SCHMID, S.M. & BRIEGEL, U. 1981: Deformation experiments on anhydrite rocks of different grain-size: rheology and microfabric. Tectonophysics 78, 527–543.
NAEF, HCH., DIEBOLD, P. & SCHLANKE, S. 1985: Sedimentation und Tektonik im Tertiär der Nordschweiz. NTB 85–14, Nagra Baden.
NOACK, TH. 1989: Computergestützte Modellierung geologischer Strukturen im östlichen Jura; Konstruktion balancierter Profile, Gravimetrie, Refraktionsseismik. PhD-thesis. Univ. Basel (unpubl.).

PLATT, J. & VISSERS, R.L.M. 1980: Extensional structures in anisotropic rocks. J. struct. Geol. 2, 397–410.

PRIESNITZ, K. 1969: Das Karstrelief des südlichen Harzvorlandes im Lichte neuerer Arbeiten zu System $CaSo_4$-$NaCl$-H_2O. Abh. 5. internat. Kongr. Speleol. (Stuttgart) M35, 1–9.

RAMEZ, M.R.H. 1976: Mechanisms of intragranular gliding in experimentally deformed anhydrite. N. Jahrb. Mineral. Abh. 127, 311–329.

RAMSAY, J. 1967: Folding and fracturing of rocks. New York (McGraw-Hill).

ROWE, K.J. & RUTTER, E.H. 1990: Palaeostress estimation using clacite twinning: experimental calibration and application to nature. J. struct. Geol. 12, 1–17.

SCHWERDTNER, W.M. 1961: Korngefügeuntersuchungen an Anhydritgesteinen im Benther Salzstock (Werk Ronneberg) bei Hannover. Kali und Steinsalz 3, 172–182.

SCHWERDTNER, W.M., VAN BERKEL, J.T. & TORRANCE, J.G. 1988: Ductile deformation of bedded anhydrite as revealed by strained nodule fabrics. Bull geol. Inst. Univ. Uppsala, N.S. 14, 64–78.

SUPPE, J. 1985: Principles of structural geology. New Jersey (Prentice Hall).

STEINER, W. 1989: Wisenbergtunnel (Bahn 2000). – in: Juradurchquerungen – aktuelle Tunnelprojekte im Jura – SIA-Dokumentation D 037, 69–80.

WIDMER, T. 1989: Stratigraphie und Sedimentologie der Anhydritgruppe (Mittlere Trias) in der Region Liestal-Arisdorf (Baselland, Nordwestschweiz). PhD-thesis Univ. Basel (unpubl.).